Available online at www.sciencedirect.com

SciVerse ScienceDirect

Scripta Materialia 67 (2012) 400–403

Scripta MATERIALIA

www.elsevier.com/locate/scriptamat

# Distribution of elastic strain in a pearlite structure

Norimitsu Koga,[a,*] Nobuo Nakada,[b] Toshihiro Tsuchiyama,[b] Setsuo Takaki,[b] Mayumi Ojima[c] and Yoshitaka Adachi[d]

[a]*Graduate Student of Engineering, Kyushu University, 744 Motooka, Nishi-ku, Fukuoka 819-0395, Japan*
[b]*Department of Materials Science and Engineering, Kyushu University, 744 Motooka, Nishi-ku, Fukuoka 819-0395, Japan*
[c]*Department of Materials Science and Engineering, The University of Tokyo, 7-3-1 Hongo, Bunkyo-ku, Tokyo 113-8656, Japan*
[d]*Department of Mechanical Engineering, Kagoshima University, 1-21-24 Korimoto, Kagoshima 890-8580, Japan*

Received 2 May 2012; revised 22 May 2012; accepted 23 May 2012
Available online 30 May 2012

Elastic strain and its distribution in a pearlite structure were visualized by means of the electron backscatter diffraction/Wilkinson method. It was found that pearlite colonies have different types of strain fields. Several mechanisms for elastic strain generation were discussed, and it was concluded that the elastic strain is mainly generated because of the lattice misfit between ferrite and cementite at the temperature at which pearlite transformation takes place.


*Keywords:* Pearlitic steel; Elastic strain; Electron backscattering diffraction; X-ray diffraction

The pearlite structure in steel is characterized by a lamellar ferrite and cementite dual-phase structure that forms a hierarchical substructure consisting of a colony and a block. The colony is defined as a region in which the directions of the cementite lamellae are identical, while the block is defined as a larger region composed of several colonies in which the ferrite matrix has an identical crystal orientation [1]. In a previous study, the authors found that a large elastic strain exists in the pearlite structure even in the as-transformed state in hypoeutectoid steels [2]. It is important to clarify the distribution of the elastic strain in pearlite quantitatively because such elastic strain might affect the mechanical properties of steels containing pearlite.

In order to evaluate the residual strain in metals, X-ray diffractometry and convergent beam electron diffractometry are generally used. X-ray diffractometry gives information about the average elastic strain within a relatively wide area of the specimen surface, but it is not suitable for analyzing a narrow local region. Convergent beam electron diffractometry, on the other hand, is the only way to measure the elastic strain in a nanoscale local region. However, this method does not give any information on the distribution of the elastic strain within the specimen. Recently, Wilkinson [3] proposed a new method to measure the elastic strain and lattice rotation in crystalline materials quantitatively by means of electron backscatter diffraction (the EBSD/Wilkinson method). This method enables high-resolution measurement of the microscopic elastic strain distribution and seems to be effective for the analysis of the elastic strain in each pearlite colony. In this study, the EBSD/Wilkinson method was employed to characterize the elastic strain in the pearlite structure of a commercial carbon steel. The mechanism for elastic strain generation in relation to pearlite transformation was then discussed.

In this study, the material used for the EBSD/Wilkinson method was a commercial hypoeutectoid steel with a chemical composition of Fe–0.55C–0.45Mn (mass%). This steel is composed of pearlite as well as proeutectoid ferrite grains with extremely low strain, and thus the reference point for the Wilkinson method can be set within the strain-free proeutectoid grain. This steel was solution-treated at 1123 K for 1.8 ks, then subjected directly to isothermal heat treatment at 953 K for 1.2 ks in order to obtain a mixed structure of pearlite and proeutectoid ferrite. In addition, a commercial hypereutectoid steel (Fe–0.9C–0.9Mn–0.4Si) with a full pearlite structure and a high-manganese hypereutectoid steel (Fe–0.8C–12Mn) were prepared for additional experiments. Since the untransformed austenite in the high-manganese steel remains even at ambient temperature without undergoing phase transformation, this steel can be used to analyze the strain and crystal rotation in the untransformed austenite

* Corresponding author. Tel./fax: +81 928022962; e-mail: koga08@takaki.zaiko.kyushu-u.ac.jp

1359-6462/$ - see front matter 
http://dx.doi.org/10.1016/j.scriptamat.2012.05.034

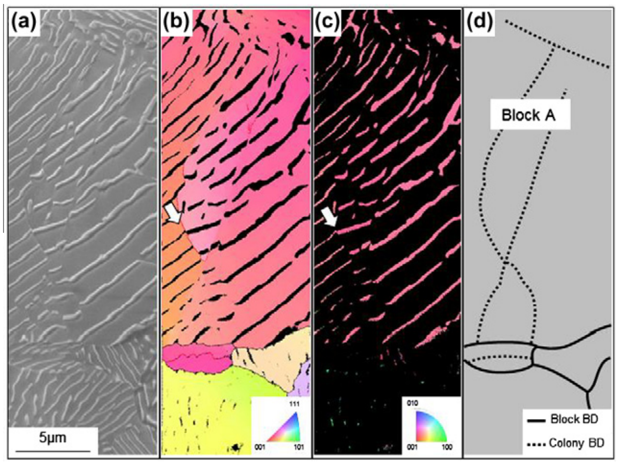


**Figure 1.** (a) SEM image of ferrite and cementite, (b) orientation-imaging map of ferrite, orientation-imaging map of cementite, and (d) microstructure map for 0.9C–0.9n–0.4Si steel isothermally transformed at 973 K.

near pearlite. The microstructure of each specimen was observed by field emission scanning electron microscopy (FESEM; JEOL-7000F, JEOL Ltd.). EBSD patterns were obtained by FESEM at an acceleration voltage of 15 kV and a step size of 0.1 μm. The obtained EBSD data were analyzed with the software programs OIM Analysis 5.31, to determine the crystal orientation, and Cross Court 3, to determine the elastic strain. In the analysis using Cross Court 3, strain and rotation tensor components are calculated separately from a small shift of the EBSD pattern between the reference and measured points. This method assumes the plate condition, which means the normal stress component, $\sigma_{33}$, is zero; however, that assumption is not strictly correct. In addition, the distortion measured at the free surface could reflect the effect of surface relaxation. The situation of the reference point should also influence the result of the analysis. From our experience, the experimental strain measured by this method seems to be overestimated, although the reason for this is unknown. Therefore, it is impossible to discuss the absolute values of strain and stress for the results of the Wilkinson method to date, and only distribution of the relative strain and stress could be evaluated in this paper. The analysis was carried out in each grain where surrounded by a high angle boundary (>15°), and the reference point was set at the center of each grain. In this article, each elastic strain tensor component is shown by color mapping.

The full width at half maximum (FWHM) of the ferrite diffraction peak was measured from the X-ray diffraction pattern obtained from an irradiated area a few millimeters in diameter. The FWHM was evaluated as the mean amount of elastic strain in a specimen. The FWHM was measured at ambient temperature as well as at the transformation temperatures.

Figure 1(a–c) shows an SEM image of ferrite and cementite, an orientation imaging map of ferrite and an orientation imaging map of cementite, respectively, for the hypereutectoid steel specimen that was isothermally transformed at 973 K. In the map shown in Figure 1(b), low angle (5–15°) and high angle (>15°) boundaries are indicated by red and black lines, respectively. The map in Figure 1(d) shows a schematic illustration of the block and colony boundaries obtained from these observations. Although there are some colonies in block A (shown in Fig. 1(d)), the maps in Figure 1(b) and (c) demonstrate that not only the ferrite phase but also the cementite phase has a similar orientation with a slight orientation graduation due to the elastic strain. However, the colony boundary has a significant misorientation, and the growth direction of cementite tends to change at the colony boundary as indicated by the arrows, which looks like the branching proposed by Hillert [4].

Figure 2(a–d) shows an SEM image, a trace of the boundaries of ferrite grains and colonies, an orientation imaging map and an elastic strain imaging map, respectively, for the shear component of elastic strain, $E_{23}$, of the ferrite phase in the hypoeutectoid steel microstructure. Proeutectoid ferrite grains can be observed at the center of the micrographs (white grains in Fig. 2(b)). The pearlite structure corresponds to the region in which lamellar contrast is observed in the map in Figure 2(a), and each colony can be clearly distinguished because

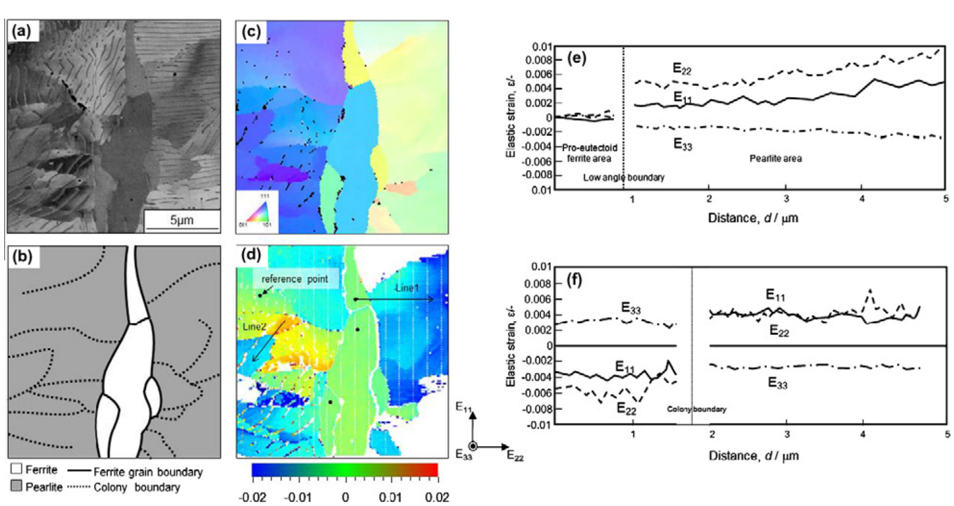


**Figure 2.** (a) SEM image, (b) microstructure map, (c) orientation-imaging map, and (d) elastic-strain map for the E23 component in 0.55C–0.45Mn stell isothermally treated at 953 K. (e) and (f) Elastic strain component profiles corresponding to lines 1 and 2 shown in (d).